

Development and Testing of Manufacturing Methods for a Piezoelectric Composite Stacked Generator
to Improve the Success Rate of Interbody Spinal Fusion

BY

Eric Tobaben

Submitted to the graduate degree program in Mechanical Engineering
and the Graduate Faculty of the University of Kansas in partial fulfillment of the
requirements for the degree of Master of Science

Dr. Elizabeth Friis, Chairperson

Dr. Kenneth Fischer, Committee Member

Dr. Ronald Barrett, Committee Member

Date Defended: 5/29/2014

The Thesis Committee for Eric Tobaben certifies

That this is the approved version of the following thesis:

Development and Testing of Manufacturing Methods for a Piezoelectric Composite Stacked Generator
to Improve the Success Rate of Interbody Spinal Fusion

Dr. Elizabeth Friis, Chairperson

Date Approved

Abstract

Interbody spinal fusion surgeries have a failure rate of approximately 10% for healthy patients. For difficult-to-fuse patients this failure rate can increase to 46%. Adjunct therapies including bone morphogenetic proteins (BMPs) and electrical stimulation have been used to increase the success rate of such surgeries. BMPs have been clinically shown to cause detrimental ectopic bone growth around the spinal cord. Current DC electrical stimulation methods have been proven to be successful, but require the use of a battery to provide power. Removing the battery after fusion has occurred requires a second surgery. A piezoelectric composite stacked generator has been developed to provide electrical stimulation to the interbody space without the need for a battery.

The piezoelectric composite was manufactured from medical grade epoxy (EPO-TEK 301) and PZT-5A1 fibers. Stacked generators require composite layers to be mechanically connected in series and electrically connected in parallel. The electrical connection of the layers provides many challenges and is the location of the most common failures. Different manufacturing methods and materials must be tested in order to find ways that reduce failure of the stacked generators. In this work, stacked generator specimens were electrically connected using copper tape with conductive adhesive (CA) and using copper tape with silver epoxy (SE).

The specimens were subjected to a 2 Hz cyclical 500 N mechanical load, across a 38 resistance load sweep (420 k Ω to 5 G Ω). This electromechanical testing regimen was performed to determine modes of failure. Electromechanical testing was conducted at three stages across the manufacturing process. Specimens were tested after being assembled and being room temperature cured (RTC), after being heat cured (HC), and after encapsulation (ENC). Voltage data was collected by measuring across the resistance load. Power was found using an average peak voltage from collected data, resistance

load, and combining Joule's Law and Ohm's Law ($P=V^2/R$). After each test, the specimen data was checked to determine whether partial or full failure had occurred.

Testing confirmed that the conductive adhesive specimens were prone to failure after HC and ENC. Only one of the original five conductive adhesive specimens was fully functional after all three tests were performed. This may be due to stress at the adhesive-epoxy interface due to HC and ENC causing mechanical and electrical failure. Silver epoxy specimens only had one specimen partially fail, but exhibited a new type of failure in the form of electrochemical migration of silver ions which led to lower power output. Future work will investigate the potential new methods of manufacturing. A conductive epoxy, such as a nickel based epoxy which does not cause failure with electrochemical migration, could be used to maintain high power output while eliminating some failure modes.

Acknowledgements

There are many people whom I would like to give thanks to for making my graduate experience as good as anyone could ask for.

- Dr. Elizabeth Friis for all her guidance and support during my graduate student career. Her drive to create and innovate products to help others has inspired everyone who has worked on this project. With her wisdom and resolution, this project has been able to get to where it is today.
- Nick Tobaben, John Domann, and Dr. Paul Arnold, the other members of the piezoelectric composite stacked generator team. Without the experience and hours of help you provided it wouldn't have been possible for the project to be where it is today. Thank you all for the work and time you invested into this project.
- Dr. Kenneth Fischer and Dr. Ron Barrett for agreeing to be a part of my thesis committee, for generously giving their time, and for their help and encouragement both with my thesis and outside of my thesis.
- The Department of Mechanical Engineering, for allowing me to continue my education at the University of Kansas and for providing a great environment for learning over the past 6 years
- Nathan Goetzinger, Kolton Stimpert, Nikki Galvis, Erin Mannen, Sami Shalhoub, Fallon Fitwater, and my friends from other labs. You've never failed to make any day in which I see you exponentially better. I look forward to seeing more of you in the future and hope we have many more board game nights to come. These last 2 years quite honestly wouldn't have been nearly as enjoyable without you all.
- Jim and Anita Tobaben and my brothers Nick and Matt. It is impossible to count how many times you have supported and encouraged me to always be the best I can. Your love and strength has helped me greatly throughout my entire life.
- Laura Stadler for being my biggest fan and friend for the last 7 years. I can't express how blessed I am to always have you to talk to and confide in. Without your constant love and support it would have been much harder to start and finish my masters.

This work was supported in part through the Institute for Advancing Medical Innovation

Table of Contents

Abstract	iii
Acknowledgements	v
Table of Contents	vi
Image List	vii
Chapter 1. Background and Significance	1
1.1. Introduction	1
1.2. Spine anatomy:	2
1.2.1. <i>The Spine</i>	2
1.2.2. <i>The Vertebrae</i>	3
1.2.3. <i>The Intervertebral Disc</i>	3
1.3. Spinal Fusion	4
1.3.1. <i>Interbody devices</i>	4
1.3.2. <i>Bone Morphogenetic Proteins</i>	5
1.3.3. <i>Electrical Stimulation</i>	5
1.4. Electrical Stimulation	6
1.4.1. <i>Inductive/Capacitive coupling</i> :	6
1.4.2. <i>Direct Current Stimulation</i>	6
1.5. General Composite Theory	10
1.6. Piezoelectric Materials.....	11
1.6.1. <i>Classical Piezoelectric model</i>	11
1.6.2. <i>Stacked generators vs. Monolithic</i>	12
1.6.3. <i>Heating Effect on Poling</i>	14
1.6.4. <i>Effectiveness of Repoling</i>	14
Chapter 2. Manuscript for Submission to Journal of Medical Devices	16
2.1. Abstract.....	18
2.3. Keywords.....	18
2.3. Introduction	19
2.4. Methods and Materials.....	21
2.5. Results.....	23
2.6. Discussion.....	23
2.7. Conclusions	26
2.8. Acknowledgements.....	26
2.9. References	27
Chapter 3. Conclusion and Future Work	32
References	34
Appendix A: Methods and Materials	36

Image List

Chapter 1. Background and Significance

Figure 1: Full spinal column (Public Domain, http://commons.wikimedia.org/wiki/File:Gray_111_-_Vertebral_column-coloured-ar.png).....	2
Figure 2: Intervertebral disc anatomy (Public Domain, http://commons.wikimedia.org/wiki/File:716_Intervertebral_Disk.jpg).....	3
Figure 3: SpF direct current stimulator, showcasing a mesh cathode.....	7
Figure 4: Speed of bone growth with various length-based current densities [19]	8
Figure 5: Unpoled (left) vs. poled (right) piezoelectric crystal (Public Domain, http://commons.wikimedia.org/wiki/File:Perovskite.svg).....	11
Figure 6: Monolithic and stacked generators © [2005] IEEE [33]	12
Figure 7: Comparison of power generated by stacked (left) and monolithic generators © [2005] IEEE [33]	13
Figure 8: Effects of heating and poling magnitude on d_{33} coefficient, a representation of the findings of Law et.al [32].....	14
Figure 9: Effect of repolling on the d_{33} coefficient of PZT 5 H© [1999] IEEE [36]	15

Chapter 1. Manuscript for Submission to Journal of Medical Devices

Figure 10: Cross sectional view of fiber-composite matrix.....	28
Figure 11: Side view of the specimen, detailing the design for electrical connection (black).....	28
Figure 12: Piezoelectric composite circuit model [11].....	29
Figure 13: Electromechanical Testing Flowchart	29
Figure 14: Power of CA method across all stages	30
Figure 15: Power of SE method specimens	30
Figure 16: Comparison of power for each conductive adhesive (CA) method specimen	31
Figure 17: Comparison of power for each silver epoxy (SE) method specimen	31

Appendix A: Methods and Materials

Figure 18: Assembled composite matrix column mold showing inside workings	37
Figure 19: Top view of the assembled column mold	38
Figure 20: Side view of the specimen, detailing the design for electrical connection (black).....	39
Figure 21: Alignment jig providing support to a stacked specimen while curing	39
Figure 22: Comparison of an initial specimen (left) and an encapsulated specimen.....	40
Figure 23: Power output for the 4th conductive adhesive (CA) method specimen across the full testing regimen	41

Chapter 1. Background and Significance

1.1. Introduction

To better understand the underlying workings of the device detailed in this thesis, a rudimentary knowledge of the spine must be obtained, including spinal anatomy and an understanding of the intervertebral disc space. Understanding the physical requirements for the device, such as the height of the specimen, is necessary and can give better insight into how the specimen is loaded while in the spine. Current spinal fusion methods need to be examined to understand the problems needing to be addressed with current methods. Current spinal fusion methods include interbody fusion cages with or without adjunct therapies such as bone morphogenetic proteins (BMPs) and electrical stimulation. Recently there have been reports of BMPs causing ectopic bone growth that extends into the spinal canal; the device discussed in the thesis will be related to electrical stimulation. The three main methods of electrical stimulation are inductive coupling, capacitive coupling, and direct current. Direct current was the selected method to encourage interbody bone growth. Direct current methods typically use a battery pack to provide an electronegative charge to the body. Battery packs are successful at supplying a DC signal to power the device. Battery packs require a second surgery to remove in cases of patient discomfort or concern. Piezoelectric materials can be used to generate a similar electrical stimulation. Piezoelectric generators are foreign to most people and therefore a basic understanding of piezoelectric theory and method of action are needed to determine the effectiveness of the generator. A piezoelectric generator turns dynamic mechanical deformations into electric charge. The power generated, along with other material properties, can be altered by using a stacked generator instead of using a single monolithic piezoelectric element. A stacked generator inhabits the same volume as a given monolithic element but is made up of piezoelectric wafers which are connected mechanically in series and electrically in parallel. An important variable in a stacked generator is the method of electrically connecting the layers. It is important to test many different methods of electrically connecting and manufacturing the stacked generator.

1.2. Spine anatomy:

1.2.1. The Spine

The spine is a complex structure found in the posterior section of the upper body that extends from the skull to the pelvis. It is comprised of 33 stacked bones called vertebrae that protect the spinal cord [1].

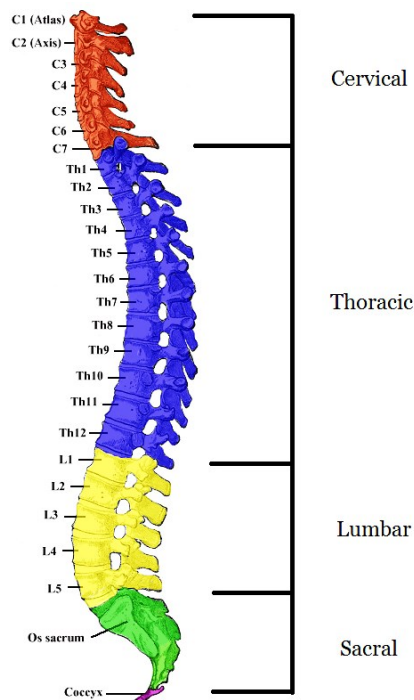


Figure 1: Full spinal column (Public Domain, commons.wikipedia.org)

There are four major regions of the spine: the cervical, thoracic, lumbar, and sacral. The cervical region contains seven vertebrae which allow for rotation and movement of the head. Directly beneath is the thoracic region. The thoracic region consists of twelve vertebrae that connect to the ribcage and helps with bending and twisting of the torso. The five vertebrae of the lumbar spine are directly inferior to the thoracic region. These vertebrae provide support for body weight while sitting or standing. The sacrum is constructed from four to five fused bones and is the foundation of the pelvis [1].

1.2.2. The Vertebrae

Most of the vertebrae found in the cervical, thoracic and lumbar regions of the spine share a similar structure. The vertebral body serves as the main load-bearing structure and is where the intervertebral discs, which connect consecutive vertebrae, attach. Posterior of the vertebrae body is the vertebral arch. The vertebral arch is made from the pedicles, laminae, and processes. The processes provide attachment sites for back muscles while the pedicles and laminae provide the structure for the spinal canal, which serves as a pathway for the spinal cord [1].

1.2.3. The Intervertebral Disc

The intervertebral discs act as shock absorbers between vertebrae. The disc consists of two main parts: the nucleus pulposus and the annulus fibrosus. The nucleus pulposus is the gel-like, viscoelastic center of the disc. The functions of the nucleus pulposus include supporting the axial loads experienced in the spine and allowing for torsional movement. The annulus fibrosus is a highly fibrous structure that surrounds and contains the high water content nucleus pulposus. It also provides the nucleus pulposus the support it needs to carry the heavy loads carried by the body. The outermost layer of each intervertebral disc is comprised of layered sheets of collagen that are offset to improve the disc's strength [1].

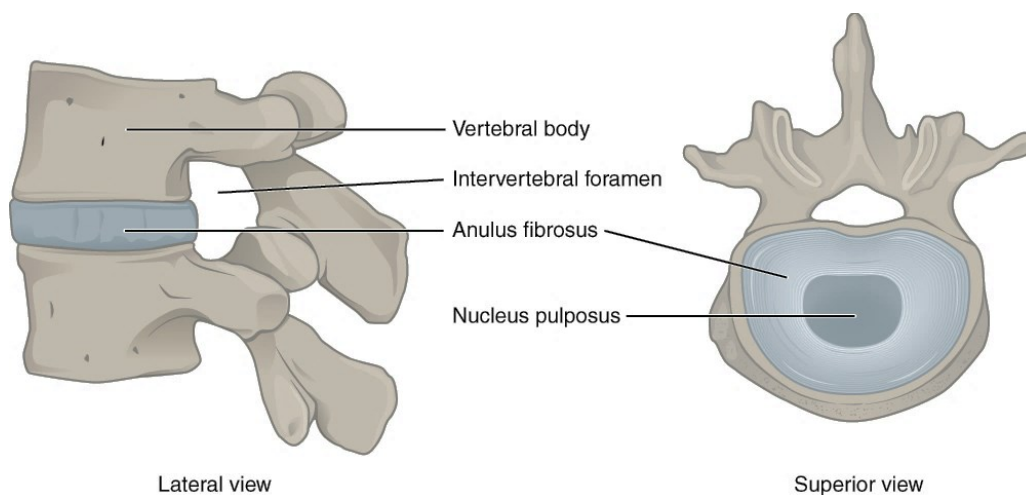


Figure 2: Intervertebral disc anatomy (Public Domain, commons.wikipedia.org)

The intervertebral discs in the lumbar region sustain the largest loads and therefore have a higher tendency to get damaged. This leads to a vast majority of the population experiencing lower back pain at some point in their life. Most of the time, back pain can be treated with exercise and medication [2]. However, in the case of degenerative disc disease, where the disc loses height and mechanical function due to becoming more fibrous, or a herniated disc, where the nucleus loses containment of its viscoelastic gel substance, surgery might be necessary [1, 3]. The surgery involves the fusion of the two vertebrae connected by the failed disc.

1.3. Spinal Fusion

1.3.1. Interbody devices

To help increase the chance of a successful spinal fusion, interbody cages are used during surgery. These devices come in many different sizes and shapes in order for a surgeon to be able to find a correct fit for any given patient. They can also be made out of many different materials; one of the most popular is titanium. When these cages are inserted into the intervertebral disc space, a pre-load is applied by the muscles. The pre-load helps ensure that the cage stays where it was placed in the body and helps the cage to provide stability [4]. The Food and Drug Administration conducted initial trials for threaded cylindrical cages. Subjects were given radiographs 2 years after their surgery to help determine how many people experienced successful fusion. The study determined that 96% of the patients had fusion. Of these, 65% had good or excellent results, 21% experienced fair fusion, and 14% had poor fusion [4]. Others have tried, but have been unable to repeat these high success rates. These devices are commonly used, are effective for single level fusion, and can be improved upon by adding pedicle screws. However, it's less certain whether fusion cages are as effective on multilevel disc degeneration/disease and other ailments.

For spinal fusion surgeries where only spinal fusion cages are used, even healthy patients have approximately a 10% chance of failure to fuse. Failure rate rises as high as 46% for difficult-to-fuse

patients, which include smokers and diabetics [5, 6]. With over 600,000 of these surgeries performed each year, there is a great need for better methods of fusion [7]. Recently, the use of adjunct therapies such as bone morphogenetic proteins (BMPs) and electrical stimulation have been used to improve success rates of surgeries.

1.3.2. Bone Morphogenetic Proteins

Bone morphogenetic proteins (BMPs) have been used with spinal fusion surgeries to promote bone growth and reduce the need of allograft. Without needing to harvest bone from the iliac crest, surgery times are able to be reduced [8]. While the exact cellular and molecular mechanisms of BMPs are not fully understood, it is known that they help with regulation osteoblast differentiation and the bone growth that is associated with it [9]. A 2-year study of 279 patients with degenerative lumbar disc disease was conducted to examine the effects of rhBMP-2 versus autogenous iliac crest bone graft on fusion. Of the study population 143 patients received rhBMP-2 and 136 received the iliac bone graft. Those that received rhBMP-2 had a quicker mean operation time and less blood loss during the surgery. After 24 months, 94.5% of the patients given BMP had fusion, compared to the 88.7% without BMP [10]. BMPs have also associated with the ectopic bone growth. A study performed by Haid et.al found that 28 of 67 patients exhibited ectopic bone extending into the spinal canal. Of these cases, 24 had been treated with BMPs. Using Fisher's exact test, the difference was determined to be statistically significant ($p < .0001$) [11].

1.3.3. Electrical Stimulation

Electrical stimulation has been used to aid in spinal fusion success. Interest in electrical stimulation greatly increased in 1957. This is when Fukada and Yasuda first presented their work on electrical stimulations effect on bone injuries [12]. Over the years, many people have conducted studies on the effects of electrical stimulation and how the body is altered by such treatments and have come up with different ideas as to how electrical stimulation works. The lack of consensus has caused confusion as to what the real mechanism of action of electrical stimulation is.

The human body reacts differently to charges caused by electrical stimulation. Electronegative fields trigger bone growth while electropositive fields result in bone resorption [13]. Upon receiving an electronegative charge, the body increases the production of specific mRNAs that are coded for growth factors. These growth factors trigger the proliferation and differentiation of cells, leading to larger bone callus and vascularization at the fusion site. By this chain of events, patients are able to recover from injuries in a shorter amount of time with fewer complications. There are three main types of electrical stimulation that are used by physicians: Inductive coupling, capacitive coupling, and direct current.

1.4. Electrical Stimulation

1.4.1. Inductive/Capacitive coupling:

Inductive coupling is a non-invasive approach where coils made from long wires are attached to a generator and placed over the fracture site, creating an electric field in the bone beneath the coils. Capacitive coupling, also a non-invasive approach, involves placing electrodes on the skin above the injury site and delivering a current from an AC generator [13]. Both of these methods increase the proliferation of osteoblasts which, with the help of calcium ions, aid in the mineralization of bone. One of the main differences is that capacitive coupling uses extracellular calcium where inductive coupling uses intracellular stores of calcium to activate the pathways that amplify the DNA events which produce the needed mRNAs. The mRNAs contain multiple growth factors, including BMP-2 and BMP-4 [14].

1.4.2. Direct Current Stimulation

Direct current stimulators are devices which are implanted in the body with cathodes that are positioned at the fracture site and an anode which is placed 5-10 cm away in soft tissue [15, 16]. A circuit is created that travels from cathode to anode through the body and creates a local current at the fracture site [13]. One example of a direct current stimulator can be seen in Figure 3. There is much confusion as to how the circuit created in the body works to promote bone growth. Some feel that the total current delivered to the cathode is what matters while others believe it is current density that

determines bone growth. There is another disagreement as to what current density is. Some feel that it is the total current per length ($\mu\text{A}/\text{cm}$) while others argue that it is total current per unit area ($\mu\text{A}/\text{cm}^2$).



Figure 3: SpF direct current stimulator, showcasing a mesh cathode

A study performed by Friedenberg et.al investigated the effects of varied total currents, distributed through a 1cm stainless steel electrode, on bone growth in rabbits. They determined that the greatest bone response occurred at 20 μA , but that above this level the presence of osteonecrosis became apparent [17]. The osteonecrosis is thought to have been caused by the stainless steel electrode receiving a current of 30 μA and the fact that stainless steel electrodes don't uniformly distribute the current. Stainless steel instead allows most of the current to leave at the insulation-wire junction resulting in higher current concentration. Titanium wire electrodes uniformly distributes the current across the electrode length and therefore don't suffer the same constraints as stainless steel when experiencing higher currents. The ability for titanium wire to successfully provide a given current density at higher current levels can be seen in an experiment conducted by Toth et.al. The study examined the effects of total current on the speed of fusion and fusion success in sheep. It was conducted with a titanium Bagby and Kuslich (BAK; Sulzer Spine-Tech, Minneapolis, MN) cage that was connected to a direct current stimulator (SpF XLII, Electro-Biology, Inc., Parsippany, NJ) which supplied varied currents to the cage. In their test they ran currents of 40 and 100 μA through the cage, which greatly exceeds the limitations found in the Friedenberg study, without witnessing any adverse effects to the body. In fact,

the largest bone growth was exhibited by the 100 μA current [18]. Another way the effect of current has been studied is by examining the effect of current density. Some groups have studied length-based current density ($\mu\text{A}/\text{cm}$) while others focused on area-based current density ($\mu\text{A}/\text{cm}^2$)

In 2001, Dejardin et.al performed a study to evaluate the effects of varied length-based current densities on spinal fusion. The current densities that were observed in the study were .83, 4, and 10 $\mu\text{A}/\text{cm}$. A current density of 10 $\mu\text{A}/\text{cm}$ was used as the max because it was near the optimal current density found from the study performed by Friedenberget et.al and was the highest density that could be created with the implantable devices being used in the study.

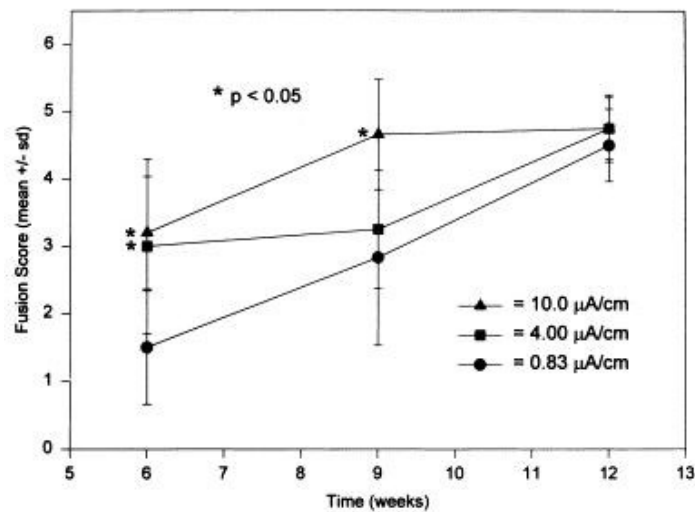
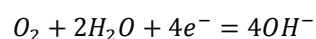


Figure 4: Speed of bone growth with various length-based current densities [19]

As can be seen in Figure 4, there is a significant statistical difference between the higher two current densities and the lower current density at six weeks. At nine weeks, the highest density is statistically significant from the other two and at twelve weeks there is no statistical significance because by that point the vertebrae had fused. Based on their results, it appears that speed of fusion can be significantly improved by increasing the direct current density towards an optimal value [19].

The final way people have studied the effect of current is with area-based current density ($\mu\text{A}/\text{cm}^2$). Simon et.al stated that from current findings, at least $1 \mu\text{A}/\text{cm}^2$ is required to promote some form of bone growth and that current density can approach $150 \mu\text{A}/\text{cm}^2$ while still being beneficial [20]. By revisiting the study performed by Toth et.al, we examine the total currents and the cathode surface area to evaluate the supplied current densities. The study supplied the cage (21.3 cm^2 surface area) with $40 \mu\text{A}$ and $100 \mu\text{A}$, yielding $1.9 \mu\text{A}/\text{cm}^2$ and $4.7 \mu\text{A}/\text{cm}^2$ respectively. Patients experiencing $1.9 \mu\text{A}/\text{cm}^2$ noticed enhanced bone growth and the patients with an area-based density of $4.7 \mu\text{A}/\text{cm}^2$ exhibited a 100% fusion incidence [18]. To determine which theory on the effect of current is correct, a better understanding of the mechanism of action for bone growth is needed.

Studies have shown that DC stimulation causes electrochemical reactions around the cathode that lead to a lower oxygen concentration and an increase in pH [21, 22]. A low oxygen content has been shown to increase cell proliferation and migration [23]. The pH change is primarily caused when electrons released by the cathode combine with water and oxygen and produce hydroxyl ions which lead to the promotion of chondrogenesis and endochondral ossification. The reaction is shown in the following equation [13].



The increased pH also aids in the bone growth process by slowing the proliferation of osteoclasts [24]. However, the change in pH doesn't fully explain the increase in bone healing. Another factor which helps is the upregulation of osteoinductive growth factors. Fredericks et.al demonstrated that direct current stimulation increases mRNA expression, especially the levels for BMP-2,6, and 7 [25]. Based on the mechanism of action, it is inferred that the correct model for direct current stimulation is using area-based current density. Area-based current density was picked because the interface where electrons can be released is reliant on surface area of exposed cathode.

1.5. General Composite Theory

Spinal fusions devices need to have high strength and toughness in order to withstand the forces generated by the body. One of the common ways spinal fusion devices deal with the forces in the body is through the use of composite materials. Composite materials have already been seen in spinal fusion devices [26]. A composite material is comprised of a matrix material and a high strength, typically brittle material in the form of a fiber or whiskers. The combination allows for the matrix material to have a higher stiffness, support the fibers to prevent buckling, and increase the toughness beyond that of the fibers alone. Controlling the fiber orientation allows a composite to better resist experienced forces. For a spinal fusion device, a unidirectional fiber layout would be justified. For a unidirectional fibrous composite, the force of compression in the direction of the fibers is transmitted through shear stress between the matrix and the fibers [27]. Therefore, the connection at the epoxy-fiber interface is very important for power generation in a piezoelectric composite.

When certain epoxies, a commonly used matrix material, are allowed to rest 24 hours at room temperature, it solidifies and appears to be fully cured. However, it has been found that heating the epoxy after allowed to solidify causes an increase in the amount of cross-linking within the epoxy matrix which in turn improves the mechanical properties of the epoxy [28]. Cross-linking generally causes a decrease in the volume of epoxy [29]. The contraction is helpful in epoxy based composites, as it improves the mechanical connection at the epoxy-fiber interface, which in turn increases the shear forces applied to the fiber during compression.

Composite design has been applied to piezoelectric generators. PZT, a type of piezoceramic, is a strong material but is brittle and prone to failure. Therefore, a composite design such as a fibrous composite is greatly beneficial as the piezoceramic is supported and less likely to fail. It has also been found that fibrous piezoelectric composites can have a greater efficiency than bulk piezoelectric ceramics [30].

1.6 Piezoelectric Materials

1.6.1. Classical Piezoelectric model

A basic definition of a piezoelectric material would be a material that either generates a charge when mechanically strained or mechanically deforms when a charge is applied. In order to understand the mechanism of action of these materials, we need to look at its microstructure. A piezoelectric ceramic is a collection of small crystals oriented in a random pattern. While the small crystals in the ceramic are piezoelectric with their own dipole moments, the material in its ordinary state is non-piezoelectric. In order to make the material piezoelectric, an electric field must be applied. The process of applying an electric field is called poling. Poling aligns the polar axes of the crystals and creates a net dipole moment. Due to the random orientation of the crystals, the poling process will create a net dipole that is less than that of the single crystal. A smaller dipole moment is created because the reorientation cannot fully align all of the crystals. The amount of alignment can be controlled by the electric field applied to the ceramic [31, 32]. Figure 5 shows the effects of poling on the perovskite crystal structure of lead zirconate titanate (PZT), a commonly used piezoelectric material.

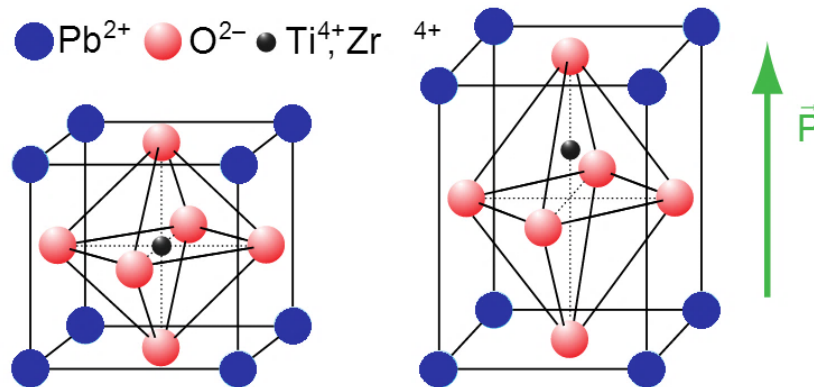


Figure 5: Unpoled (left) vs. poled (right) piezoelectric crystal (Public Domain, commons.wikipedia.org)

1.6.2. Stacked generators vs. Monolithic

There are two main types of piezoelectric power generators that are used for through-thickness loading: a single monolithic generator and a stacked generator. To understand why one would be better in a given application, knowledge on how size and shape of piezoelectric elements affect the generator's power output must be obtained. First, mechanical stress is related to cross sectional area. Next, the voltage produced is related to the stress on the element. Finally, the charge displacement is related to the volume of the element. For similar generators, the main differences between a stacked generator and a monolithic generator are the changes in open circuit voltage and effective capacitance. The impact and differences of using a stacked generator instead of an equal height solid sample specimen was investigated by Platt et.al [33]. Platt compared two PZT piezoelectric generators: a 1 cm diameter, 2 cm long homogenous monolithic generator and a stacked generator of equal dimensions but consisting of ~145 PZT wafers (Figure 6). These wafers are mechanically attached in series but electrically connected in parallel.

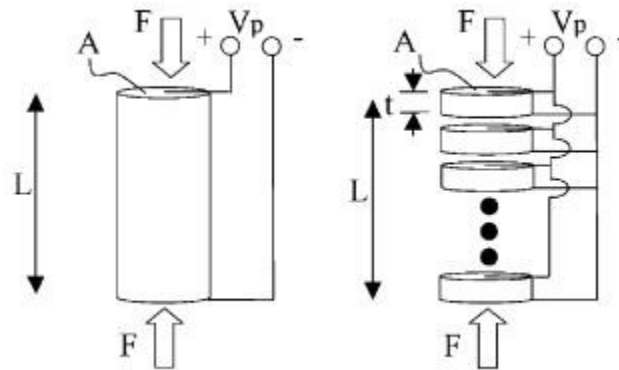


Figure 6: Monolithic and stacked generators © [2005] IEEE [33]

For the single element generator, an open circuit voltage of ~10,000 V was observed with a capacitance of ~47 pF. In comparison, the stacked generator had a much lower open circuit voltage at only ~30 volts, but also boasted an effective capacitance of 1-10 μ F. After undergoing testing with the same loading conditions, it is clear to see the difference caused by using a stacked generator (Figure 7).

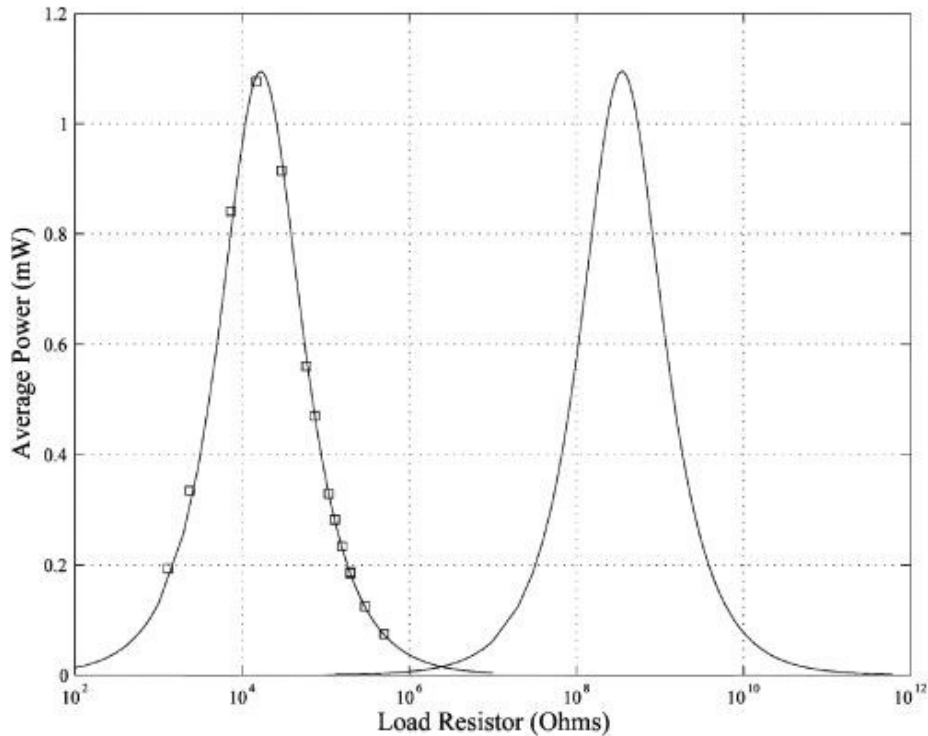


Figure 7: Comparison of power generated by stacked (left) and monolithic generators © [2005] IEEE [33]

The power generation of the two types is the same, but occurs at different load resistances. The resistance load to achieve the same max power is in the kΩ range for the stacked compared to the GΩ value for the monolithic element. Stacked elements are preferred for most applications since there is a lower matching electrical load required. The higher capacitance of the stacked generator also is important for energy transfer [33]. However, it is much harder to manufacture stacked generators as every slice has to be electrically and mechanically connected. For instance when connecting the layers together mechanically, if they are not perfectly parallel the individual layers could be producing out-of-sync signals which lower the total power generated [34]. Therefore, it is important to determine whether it is worth using a stacked generator over a monolithic element for any given design.

1.6.3. Heating Effect on Poling

With current manufacturing methods, it is important to understand the effects of heat on poled PZT fibers. A study looking into the heating effect on PZT was performed by H. H. Law in conjunction with 2 universities in Australia. Their research was conducted to find the relationship between domain orientation and piezoelectric properties after various thermal treatments were administered. Figure 8 is a representation of the results presented by Law. Poling of the PZT increases the piezoelectric constant d_{33} which in turn leads to an increase in the materials g_{33} , the piezoelectric voltage constant. The d_{33} value increases to a maximum when an electric field of 2 kV/mm is applied. They found that as the PZT is heated past 100 °C the d_{33} constant decreases until approximately 300°C where the PZT completely loses its piezoelectric properties [32].

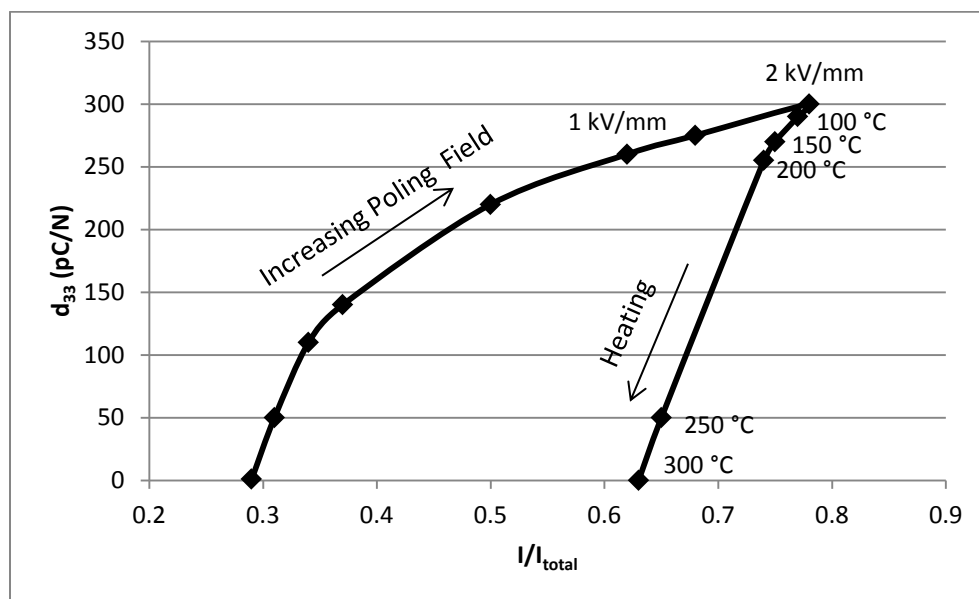


Figure 8: Effects of heating and poling magnitude on d_{33} coefficient, a representation of the findings of Law et.al [32]

1.6.4. Effectiveness of Repoling

As a piezoelectric generator is loaded and unloaded during electromechanical testing, it is very likely for the stresses applied to reorient the individual piezoelectric crystal dipole moments [35]. The gradual reorientation of dipole moments can lead to a depoling of the generator over time. A study by

Q. Zhang et.al investigated how the properties of PZT changed under the influence of mechanical stresses. They found that PZT has a memory of its original poling direction. Once the PZT has become slightly depoled, it can be repoled to its original high polarization level by applying an electric field, even smaller than originally applied, to the ceramic as long as it is parallel to the original poling direction [36].

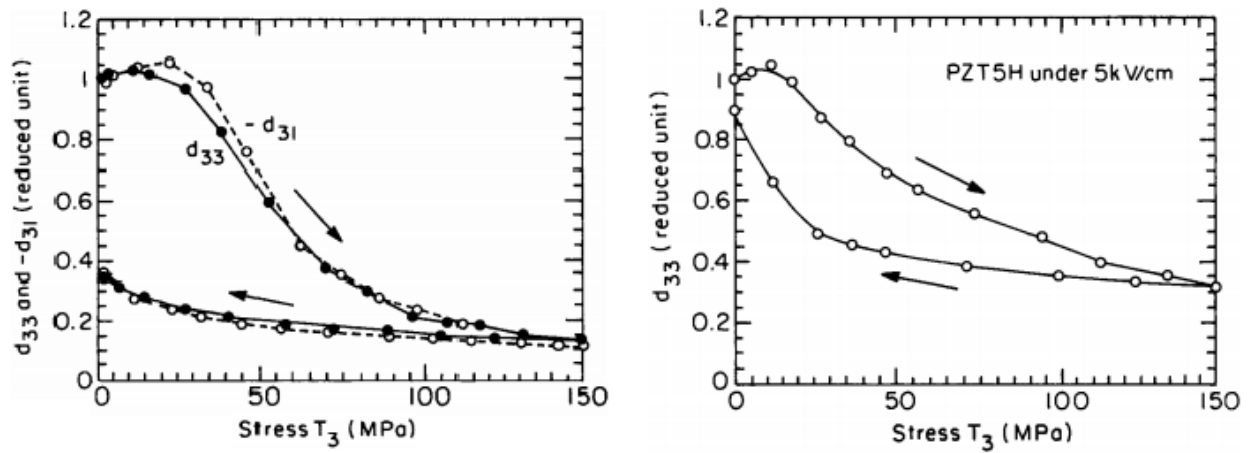


Figure 9: Effect of repoling on the d_{33} coefficient of PZT 5 H0 [1999] IEEE [36]

Chapter 2. Manuscript for Submission as a Technical Note to a Peer-Reviewed Journal

This manuscript in Chapter 2 is in the form of a manuscript that will be submitted as a Technical Note to a peer-reviewed journal in the field of smart materials. It details the testing of two manufacturing methods of a piezoelectric composite stacked generator. The paper explains the testing regimen used to determine the success of each manufacturing method, which in turn helps to outline pitfalls with the currently used methods. The references used in the manuscript are considered separate from those of the thesis body.

Piezoelectric composite stacked generator for increased interbody spinal fusion success: Experimental effects of manufacturing method on electrical stimulation potential

Eric J. Tobaben
Department of Mechanical Engineering,
University of Kansas
Lawrence, Kansas 66045

Nathan C. Goetzinger
Department of BioEngineering
University of Kansas
Lawrence, Kansas 66045

John P. Domann
Department of Mechanical Engineering
University of Kansas
Lawrence, KS 66045

Ronald Barrett-Gonzales
Department of Aerospace Engineering
University of Kansas
Lawrence, KS 66045

Paul M. Arnold
Department of Neurosurgery
Kansas University Medical Center
Kansas City, Kansas 66160

Elizabeth A. Friis
Department of Mechanical Engineering,
University of Kansas
Lawrence, Kansas 66045

Corresponding Author:

Lisa Friis, lfriis@ku.edu, Associate Professor, Mechanical Engineering, University of Kansas, 1530 W. 15th St., 3138 Learned Hall, Lawrence, KS 66045

2.1. Abstract

A piezoelectric composite stacked generator was developed to promote bone growth in spinal fusion surgeries. The objective of this study is to examine a method of manufacturing using conductive adhesive copper tape and compare to an alternative method using silver epoxy. Furthermore, this work investigates potential modes of failure and the ability of the specimen to provide an adequate amount of power for electrical stimulation. Three testing stages were conducted to determine potential failure mechanisms. It was determined that the silver epoxy method improved one failure mode but decreased power output and introduced detrimental silver ion migration.

2.3. Keywords

Electrical stimulation, spine, fusion, piezoelectric, stacked generator

2.3. Introduction

Lower back pain is one of the major reasons for physician office visits in the USA. The most serious, persistent cases of lower back pain are often treated by spinal fusion surgery which provides stability to the spine through the fusing of adjacent vertebrae. Spinal fusion surgery is performed over 600,000 times annually [1]. Of these treatments, failure to fuse has been shown to occur in approximately 10% of healthy patients with the rate rising as high as 46% for difficult-to-fuse populations, including smokers and diabetics [2, 3]. Patients who experience a failure to fuse must endure ongoing pain and require a costly and difficult revision surgery.

The current method of treatment is the use of a spinal fusion interbody device (cage) which is placed in the intervertebral space and stabilizes the spine. For the difficult-to-fuse patient population, adjunct therapies have been used clinically to address the high potential rate. These adjunct therapies are used as a supplement to the standard interbody device. The most widely used of these therapies are bone morphogenetic proteins (BMPs) and electrical stimulation. BMPs have been shown to help enhance bone healing and increase spine fusion rates [4, 5]. However, BMPs have also been shown to cause ectopic bone growth, which can be detrimental to patients particularly in the area near the spinal cord [6]. Electrical stimulators generate electromagnetic fields to provide increased bone healing and can be used both internally and externally. While being non-invasive, external electrical stimulators have user compliance issues as patients are required to wear the devices for a given number of hours each day. Internal electrical stimulators are invasive (implantable) devices which provide direct current (DC) stimulation to an electrode; bone growth is promoted in a radius of 5-8 mm from the electrode [7]. Current clinically available DC stimulation electrodes are not approved for placement in the interbody space but instead provide stimulation to titanium electrodes positioned posterior to the transverse processes. The current is supplied by an implantable battery pack placed in the soft tissue 5-10 cm away from the electrodes [8, 9]. While these devices have been clinically shown to increase fusion success, there are drawbacks to using such a method. This includes not being able to provide stimulation directly

to the interbody space where the bone fusion is desired and most mechanically effective, using a battery pack to provide stimulation, and the likelihood of a second surgery to remove the battery pack because of patient discomfort or concern.

To improve upon these existing therapies, it was apparent there was a need for a device that could deliver DC stimulation without the use of a battery pack. This led to the use of piezoelectric materials in a spinal fusion interbody device. Piezoceramics produce electric charge when mechanically strained through dynamic loads. Through cyclic loading and the use of a rectifying circuit, a DC voltage could be generated by the natural loading and unloading of the spine. That voltage could be used for supplying DC current for electrical stimulation to an electrode directly mounted on the interbody device, thus promoting fusion across the interbody space.

Piezoelectric monolithic generators and stacked generators have been used in many high-frequency applications to provide power generation, but have only found limited use in the body. The limited use is due in part to the high voltage, low current, and high impedance characteristics of piezoceramics that are not conducive to low frequency power generation applications. Piezoceramics are also brittle and very stiff which can lead to mechanical failure in the body [10]. Through the use of stacked generators, the impedance of the piezoelectric can be shifted to more closely match impedance levels found in the body, allowing for increased power generation from the same applied mechanical loads. The toughness of a piezoelectric device can be improved through the use of a piezoelectric ceramic fiber composite with a tough polymeric matrix. In the present study, mechanically and biologically biocompatible composite materials have been developed that could be used in a spinal fusion device that is in the form of a stacked generator to lower impedance [11]. The techniques for adhering the composite layers of the stacked generator must be developed and tested.

The objective of this work is to compare two methods of manufacturing piezoelectric composite stacked generators that could be used as the inner portion or insert of a spinal fusion implant. Potential

modes of failure and the ability of the implant insert to provide an adequate amount of power for electrical stimulation are also examined.

2.4. Methods and Materials

Piezoelectric composite columns, approximately 100 mm tall and with a fiber volume fraction of 30%, were manufactured from medical grade epoxy (EPO-TEK 301, Epoxy Technology Inc., Billerica, MA) and 800 micron diameter, 150 mm long PZT-5A1 fibers (Smart Materials Corp., Sarasota, FL) using a customized stainless steel mold. The design of the mold provided the desired geometry and allowed proper fiber alignment along the length of the column, providing even spacing so there was not interference between fibers (Figure 10). Using a diamond saw, 3 mm thick slices were cut from the composite columns. Electrodes were created on the top and bottom surfaces of the specimen slices using a 100 nm thick gold sputter-coated layer. Three of these slices were electrically connected in parallel and then mechanically connected in series with epoxy, as illustrated in Figure 11.

Two methods were tested for connecting the layers. In the first method, the layers were electrically connected using copper tape with conductive adhesive (CA) (McMaster-Carr, Item #76555A641). In the second method, the layers were connected using copper tape (with adhesive removed) and silver epoxy (SE) (EPO-TEK H20E, Epoxy Technology Inc., Billerica, MA). The silver epoxy was used to mechanically and electrically connect the copper tape to the composite layers. After all materials had cured, the layered specimens were then immersed in an oil bath and poled with an electric field of 1 kV/mm for 30 minutes using a high voltage power supply (Trek, Model 10/10B-HS, Lockport, New York). After poling, the specimens were given a 30 minute rest period before electromechanical testing.

The specimens were electromechanically tested using an MTS Model 858 Mini Bionix II (MTS Corp., Eden Prairie, MN) with a self-aligning platen. They were tested under cyclic loading at a frequency of 2Hz, a mechanical load of 500N, and across 38 electrical resistance loads ranging from 420 k Ω to 5

GΩ. The frequency and mechanical load were chosen to represent the approximate levels experienced during an average adult's natural walking gait [12-14]. The theoretical model developed by Tobaben et.al provided the model for the testing procedure (Figure 12) [11]. The voltages were measured across the load resistance. The raw voltages generated by the layered specimens were collected at 512 Hz into text files and were subsequently analyzed with MATLAB. Local peaks in the voltage were found by shifting the voltage offset to 0 V and rectifying the data. The data was truncated so that the first 2.5 cycles and the last 2.5 cycles were eliminated to remove any data spikes caused by the initial loading and the final unloading. An average peak voltage was found by taking the average of the remaining peaks. Average peak power for each resistance was then calculated by using the average peak voltage, the resistance value, and by combining Joule's Law and Ohm's Law ($P=V^2/R$).

As illustrated in Figure 13, electromechanical testing was performed on the specimens made with the two different layer adhesion techniques (CA and SE) at each of the three stages of manufacturing: (1) room temperature cure (RTC), (2) heat cure (HC), and (3) encapsulation (ENC). Specimens were poled after each stage of manufacturing and allowed to rest for 30 minutes prior to electromechanical testing. The silver epoxy (SE) specimens did not undergo RTC testing because the technique requires a heat treatment to cure the silver epoxy. After RTC testing, the CA specimens underwent the manufacturer's recommended heat treatment to finish epoxy cure (HC). The CA specimens were heat treated at 65°C for at least 1 hour and the SE specimens were treated at 120°C for at least 1 hour (the requirement for curing silver epoxy). All specimens were allowed to cool to room temperature before poling and electromechanical testing. The specimens (CA and SE) were then subjected to an encapsulation process (ENC). During this process, wires were connected to the positive and negative terminals of the specimen to allow both poling and the measurement of power after encapsulation. Wired specimens (CA and SE) were then placed in an encapsulation mold, surrounded in epoxy (as would be done for a usable, implantable spinal fusion device) and heat treated at 65°C for at

least 1 hour. Encapsulated specimens were cooled to room temperature, poled, and electromechanically tested. The measured voltages and calculated powers from these tests (RTC, HC, ENC) were compared to elucidate sources of concern in both methods.

2.5. Results

Power output from the specimens is the measure that can be most easily compared to different electrode configurations of clinically available bone stimulation devices. Figure 14 displays the power generated by the individual specimens from the CA method at each stage of testing. Specimens CA 1 and 2 show a trend of decreasing power by approximately 30% after heating while specimens CA 3-5 show a substantial increase approximately doubling the power output after heating. The available power decreased in all samples after the specimens were encapsulated. Figure 15 gives the available power generated by the SE method specimens for stages 2 and 3 of testing. Specimens SE 1 and 2 show a decrease in power by about 62% and 28% respectively when encapsulated. Specimens SE 3 shows an increase of approximately 560%.

Figure 16 shows a comparison of power generated by each CA specimen over the full resistance load range. This comparison allows for the identification of resistance load level at which peak power occurs. Peak power is found at an average of $1.55 \times 10^8 \Omega$ for the CA method specimens. There is evidence of a shift in optimal load resistance in CA 2 and 3 from $1.55 \times 10^8 \Omega$ to $5.03 \times 10^8 \Omega$ and $5.03 \times 10^8 \Omega$ after heat cure and encapsulation, respectively. Figure 17 compares the available power generated by each SE method specimen across the 38 resistance load range. Evidence of a shift in optimal load resistance $1.70 \times 10^8 \Omega$ to $5.03 \times 10^8 \Omega$ from heat cure to encapsulation can be seen in SE 1.

2.6. Discussion

Power output from the specimens is integral to the success of electrical stimulation aided spinal fusion. It is very important to understand the changes in power both between the different stages of

testing, between the individual specimens of a given manufacturing method, and between the methods of specimen manufacturing.

The transition from before heating to after heating can only be seen in the CA specimens. CA 1 and 2 have a decrease in power while CA 3-5 have an increase after heating. The increase after heat cure is attributed to the properties and mechanism of curing epoxy and the method of loading on the fibers in a fibrous 1-3 composite. As room temperature cured epoxy is heated, the amount of crosslinking in the epoxy increases which causes a contraction of the epoxy [15, 16]. Pogany et.al examined this phenomenon in 1968 using internal friction and creep measurements of an epoxy resin. They noted how curing at elevated temperatures caused a secondary relaxation, signaling a continuation of crosslinking and the reduction of unreacted epoxy and amine groups which are found in epoxies cured below 25 °C [15]. Contraction of epoxy generates a greater transverse force on the composite fibers which in turn increases the epoxy-fiber interface shear force applied to the fibers during compression. Fibers in a composite are loaded through shear forces applied by the matrix, thus the contraction of epoxy would be expected to increase the power generated [17]. The epoxy contraction can also accentuate flaws in the CA method, specifically at the adhesive-epoxy interface. Flaws at the adhesive-epoxy interfaces can cause complications with the electrical connectivity of the layers, leading to lower power output. Power loss can also come from repetitive testing of and cyclic failure of the bond sites and/or surface electrode integrity.

A drop in power is seen after the encapsulation process had been conducted. The lower power was expected because the encapsulation process increases the total surface area of the specimen, leading to a decrease in the stress applied by mechanical loading. Lower stress leads to less fiber compression and less power generated. The only specimens that did not share this trend were CA 5 and SE 3. Specimen CA 5 was mechanically damaged during removal from the encapsulation mold, and SE 3 showed an increase in power over the extraordinarily low power generated by its HC test.

A shift in the resistance load at which peak power is obtained can be seen for specimens of both manufacturing methods. It is noticeable for CA 2, CA 3, and SE 1 as can be seen in Figure 16 and Figure 17. The layers of the specimens are electrically connected in parallel, so the increase in resistance indicates the loss of connectivity of 1 or more layers. The loss of layers explains the drastic loss of power evident in specimen CA 3.

A comparison of Figure 14 and Figure 15 shows a distinct difference between the CA and SE manufacturing methods. The CA method specimens have a much higher available power than the SE method. The power shift is mostly likely caused by the 2nd method's manufacturing process and the method for electrical connection. Silver epoxy was used to connect the layers to remove the failure mode caused by using conductive adhesive but, due to the electrical failure mechanics present in silver, ended up causing an entirely new failure mode. It has been shown that silver ions move from anode to cathode and in our case could travel across the length of the PZT fibers themselves. The accumulation of these silver ions on the cathode results in bridges between anode and cathode, known as dendrites, which significantly decreases the surface insulation resistance in a process called electrochemical migration (ECM) [18, 19]. ECM failure rate is dominated by silver ion generation and is correlated to temperature, with higher temperatures increasing failure rate [18]. The use of silver epoxy also created problems with keeping the specimen layers parallel with respect to each other which can lead to the individual layers producing power out of phase and a lower power output. However, it is worth pointing out that of the four CA specimens to undergo all three testing conditions, CA 1 and 2 completely failed, CA 3 lost the use of 1 or more of its layers, and only CA 4 remained intact. The SE method specimens exemplified similar features with SE 1 losing 1 or more of its layers, SE 2 remaining intact, SE 3 showing signs of failed testing or failure caused by manufacturing method and method of electrical connection, but no specimens failed completely.

2.7. Conclusions

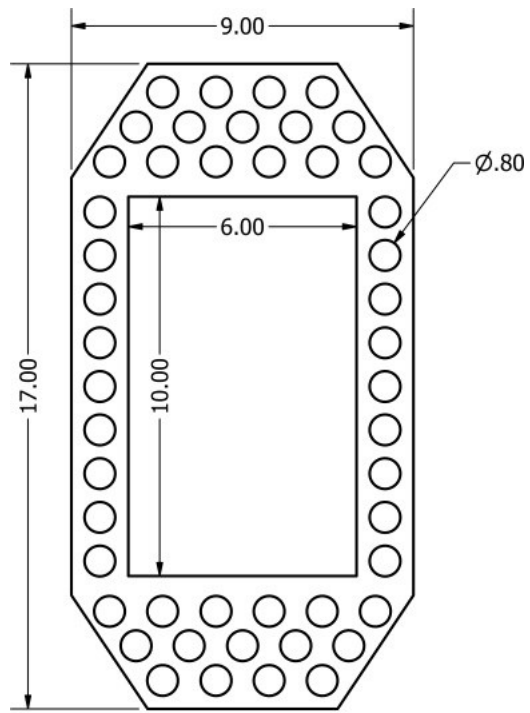
Investigating and eliminating modes of failure is of the utmost importance when a device like this is being designed. The testing regimen carried out in this work made it clear that there were many issues with the CA and SE manufacturing method. These problems manifested themselves at the electrical connection interface with the manufacturing style and material choice for electrical connection between layers. Copper tape with conductive adhesive allowed for an easy and repeatable manufacturing technique and silver epoxy helped eliminate complete failures from heating or encapsulating. Future work will investigate designs to marry these two manufacturing techniques to maintain high power output while eliminating failure modes. This could potentially be done with a Nickel based conductive epoxy for the material because it does not have the failure mode associated with the mobility of silver ions.

2.8. Acknowledgements

This research was supported by the Institute for Advancing Medical Innovation. The authors would also like to thank Michael Latham for his assistance in specimen preparation and manufacturing.

2.9. References

- [1] Spine-Health, 2009, "Spinal Fusion Surgery Worth the Cost for Stenosis Patients," <http://www.spine-health.com/blog/spinal-fusion-surgery-worth-cost-stenosis-patients>.
- [2] KANE, W. J., 1988, "Direct current electrical bone growth stimulation for spinal fusion," *Spine*, 13(3), pp. 363-365.
- [3] Gan, J. C., and Glazer, P. A., 2006, "Electrical stimulation therapies for spinal fusions: current concepts," *European Spine Journal*, 15(9), pp. 1301-1311.
- [4] Gautschi, O. P., Frey, S. P., and Zellweger, R., 2007, "Bone morphogenetic proteins in clinical applications," *ANZ journal of surgery*, 77(8), pp. 626-631.
- [5] Burkus, J. K., Gornet, M. F., Dickman, C. A., and Zdeblick, T. A., 2002, "Anterior lumbar interbody fusion using rhBMP-2 with tapered interbody cages," *Journal of spinal disorders & techniques*, 15(5), pp. 337-349.
- [6] Haid Jr, R. W., Branch Jr, C. L., Alexander, J. T., and Burkus, J. K., 2004, "Posterior lumbar interbody fusion using recombinant human bone morphogenetic protein type 2 with cylindrical interbody cages," *The Spine Journal*, 4(5), pp. 527-538.
- [7] Simon, J., and Simon, B., 2008, "Electrical bone stimulation," *Musculoskeletal Tissue Regeneration*, Springer, pp. 259-287.
- [8] Kahanovitz, N., 2002, "Electrical stimulation of spinal fusion: a scientific and clinical update," *The Spine Journal*, 2(2), pp. 145-150.
- [9] Shellock, F. G., Hatfield, M., Simon, B. J., Block, S., Wamboldt, J., Starewicz, P. M., and PUNCHARD, W. F., 2000, "Implantable spinal fusion stimulator: assessment of MR safety and artifacts," *Journal of Magnetic Resonance Imaging*, 12(2), pp. 214-223.
- [10] Platt, S. R., Farritor, S., and Haider, H., 2005, "On low-frequency electric power generation with PZT ceramics," *Mechatronics, IEEE/ASME Transactions on*, 10(2), pp. 240-252.
- [11] Tobaben, N. E., Domann, J. P., Arnold, P. M., and Friis, E. A., 2013, "Theoretical model of a piezoelectric composite spinal fusion interbody implant," *Journal of Biomedical Materials Research Part A*.
- [12] Walpole, S. C., Prieto-Merino, D., Edwards, P., Cleland, J., Stevens, G., and Roberts, I., 2012, "The weight of nations: an estimation of adult human biomass," *BMC Public Health*, 12(1), p. 439.
- [13] Kumar, N., Judith, M. R., Kumar, A., Mishra, V., and Robert, M. C., 2005, "Analysis of stress distribution in lumbar interbody fusion," *Spine*, 30(15), pp. 1731-1735.
- [14] Cromwell, R., Schultz, A. B., Beck, R., and Warwick, D., 1989, "Loads on the lumbar trunk during level walking," *Journal of Orthopaedic Research*, 7(3), pp. 371-377.
- [15] Pogany, G., 1969, "The β -relaxation in epoxy resins; the temperature and time-dependence of cure," *Journal of materials science*, 4(5), pp. 405-409.
- [16] Jeong, U., Ryu, D., Kim, J., Kim, D., Russell, T. P., and Hawker, C. J., 2003, "Volume contractions induced by crosslinking: a novel route to nanoporous polymer films," *Advanced Materials*, 15(15), pp. 1247-1250.
- [17] Hyer, M. W., 2009, *Stress analysis of fiber-reinforced composite materials*, DEStech Publications, Inc.
- [18] Yang, S., and Christou, A., 2007, "Failure model for silver electrochemical migration," *Device and Materials Reliability, IEEE Transactions on*, 7(1), pp. 188-196.
- [19] DiGiacomo, G., "Metal migration (Ag, Cu, Pb) in encapsulated modules and time-to-fail model as a function of the environment and package properties," *Proc. Reliability Physics Symposium, 1982. 20th Annual, IEEE*, pp. 27-33.



All units are in mm

Figure 10: Cross sectional view of fiber-composite matrix

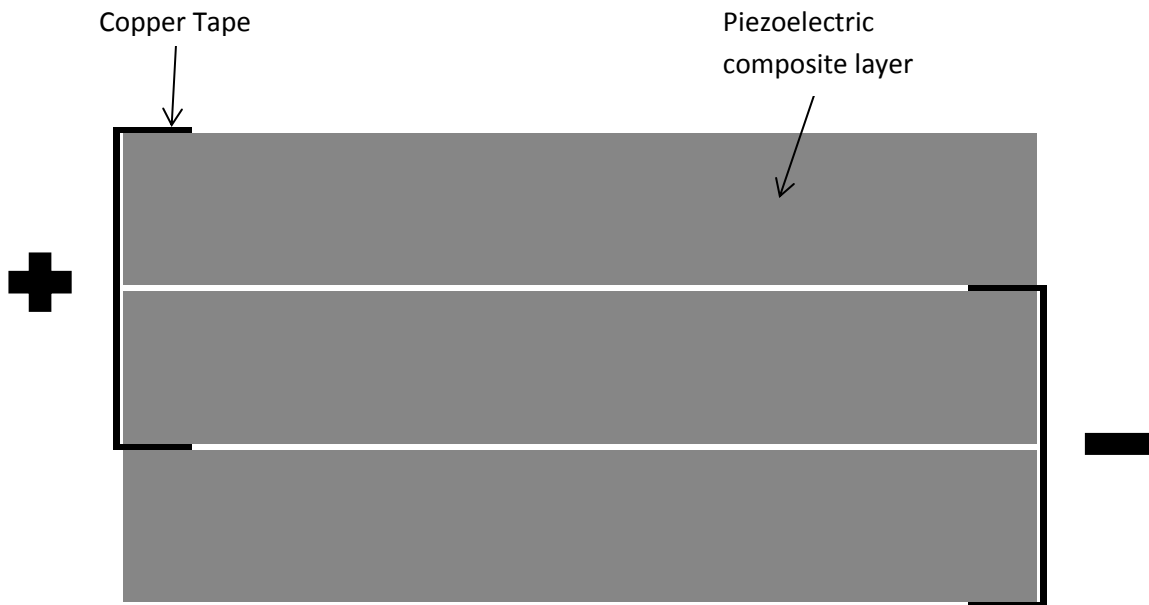


Figure 11: Side view of the specimen, detailing the design for electrical connection (black)

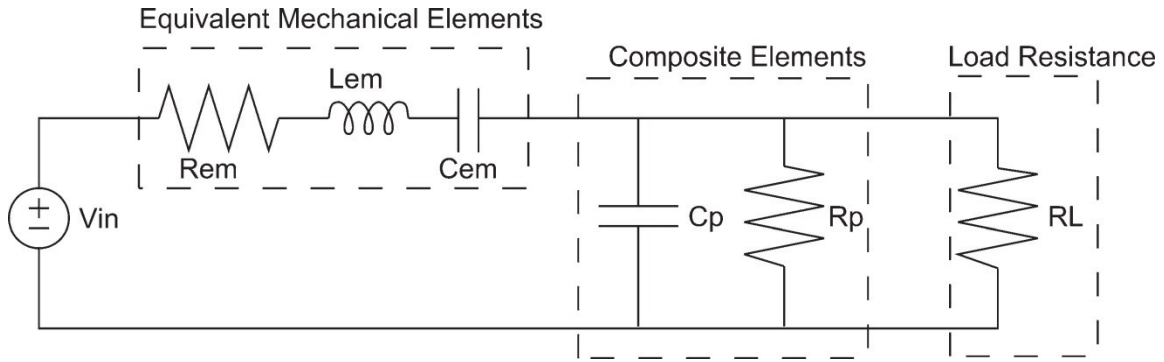


Figure 12: Piezoelectric composite circuit model [11]

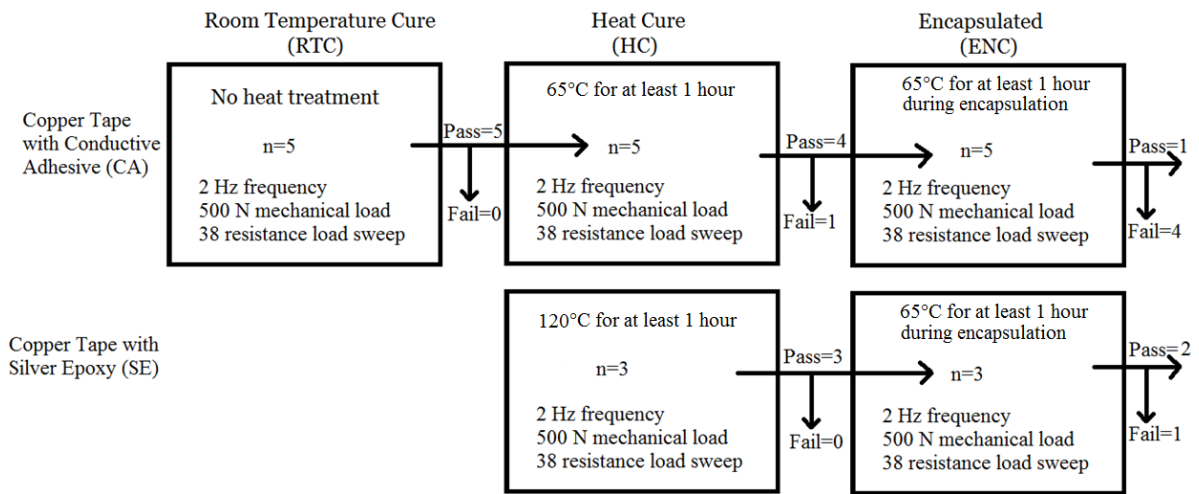


Figure 13: Electromechanical Testing Flowchart

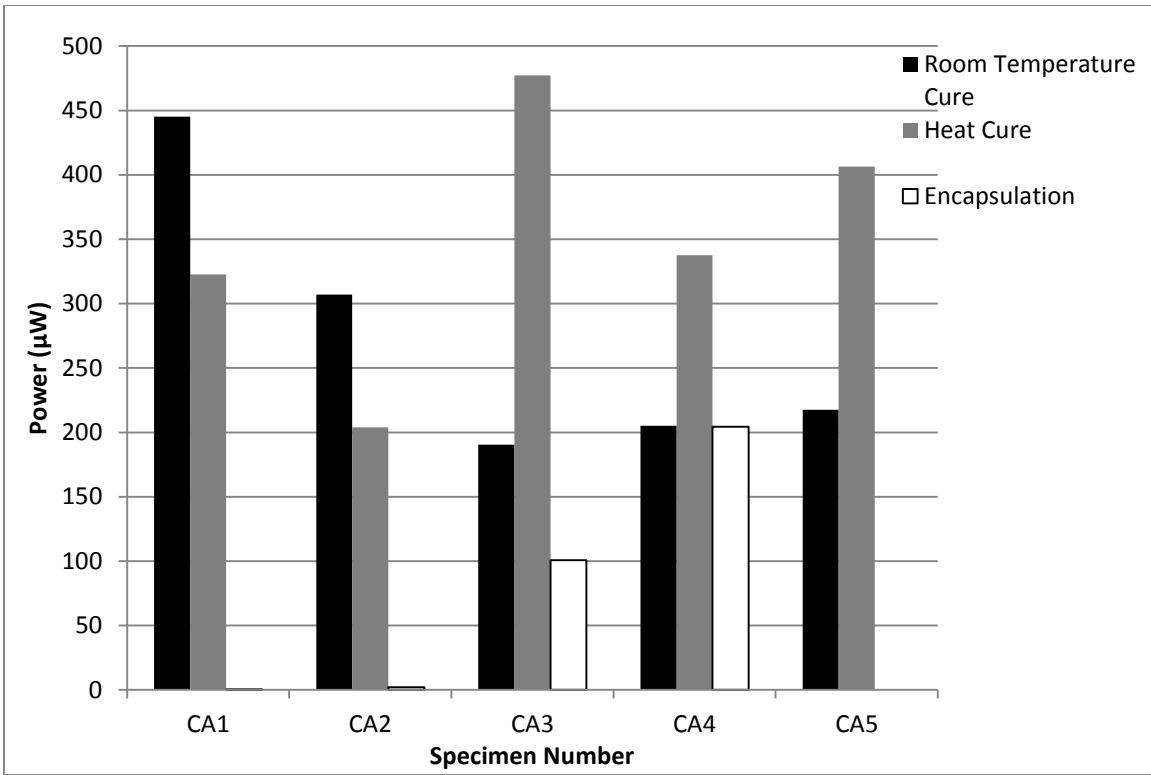


Figure 14: Power of CA method across all stages

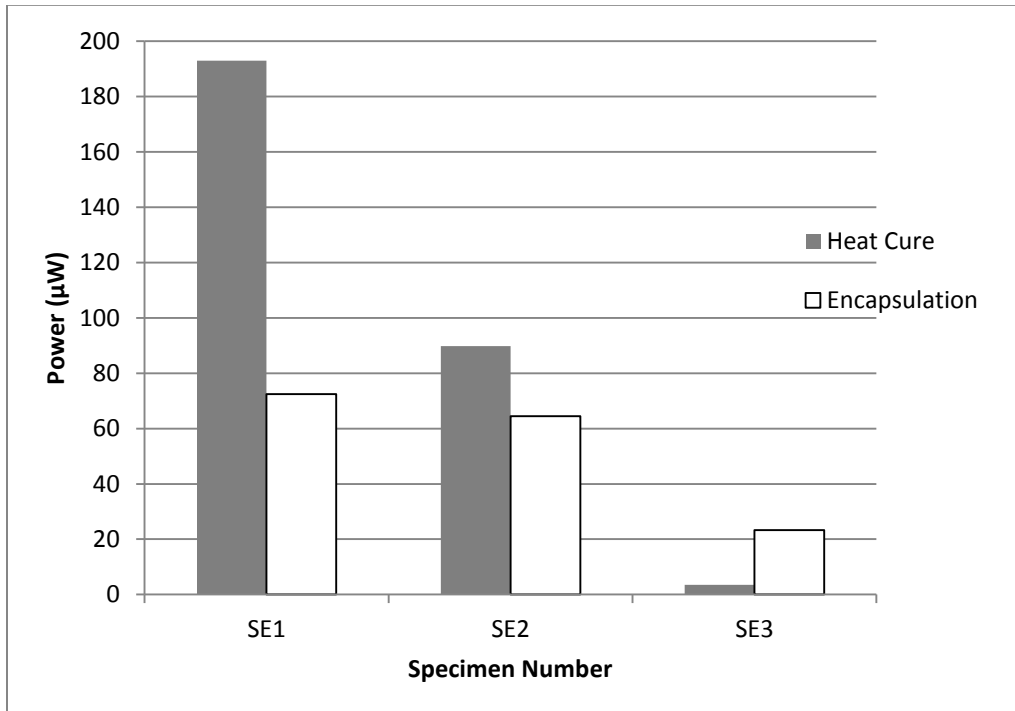


Figure 15: Power of SE method specimens

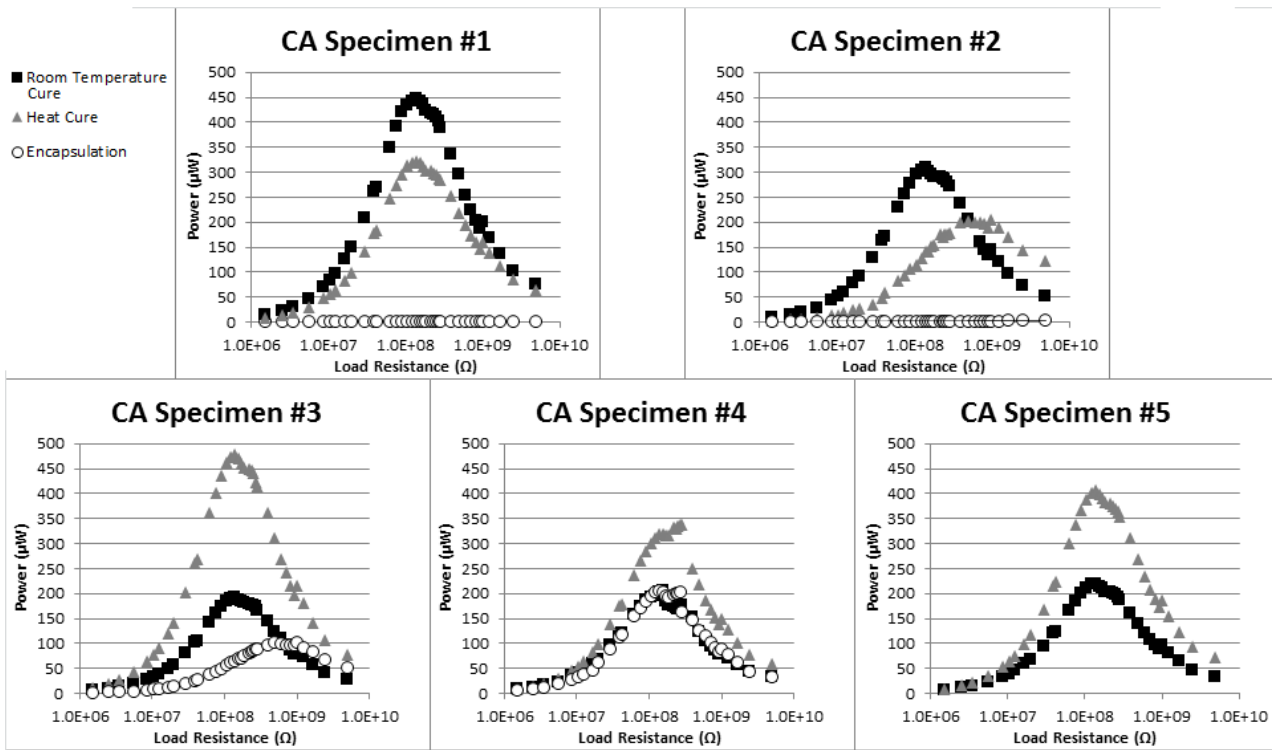


Figure 16: Comparison of power for each conductive adhesive (CA) method specimen

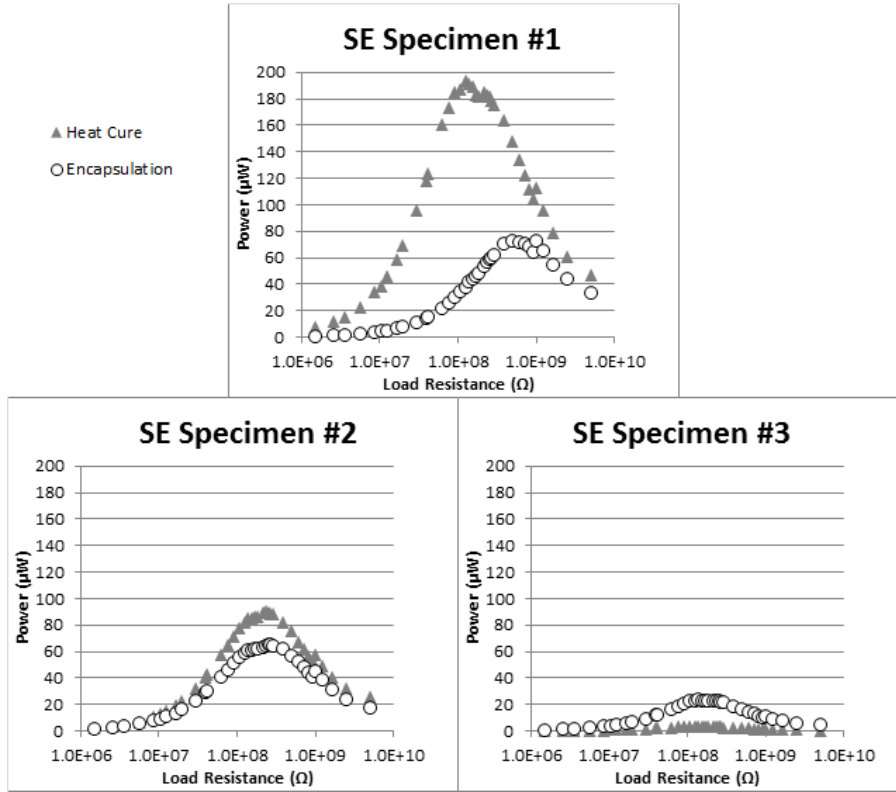


Figure 17: Comparison of power for each silver epoxy (SE) method specimen

Chapter 3. Conclusion and Future Work

Testing modes of failure is necessary when developing an implantable medical device. The studies performed clearly indicate that the two current methods are not fit for the final specimen design. The CA specimens provided adequate power but also suffered from its electrical connection method which led to 2 of 4 specimens completely failing and another 1 losing connection to 1-2 layers of the specimen. The SE specimens generated less power but showed no sign of full failure. However, 1 of the SE specimens showed signs of losing connectivity to 1-2 layers. The SE specimen data failed to show a consistent trend throughout all specimens leading us to believe that there were other problems present in this method. The current issues that need to be addressed are the materials chosen for electrical connection and the manufacturing method. The results from the CA specimens and SE specimens showed that copper tape with conductive adhesive and silver epoxy, respectfully, are not ideal materials to use for electrical connection and can cause electrical failure at the copper tape-layer interface. Silver epoxy can cause failure through the generation and migration of silver ions. Additionally, the SE specimens exhibited a poor manufacturing method that caused the specimen layers to not be parallel and for compressive forces to not be evenly distributed.

In order to correct the current failings in the manufacturing process, more research must be done to find a way of combining the successes of each method while eliminating their downsides. The SE method shows promise in that complete failure of a specimen wasn't noticed in the 3 samples. If a method like such is to be used, a different bonding agent would be needed to eliminate the failure caused by the mobility of metal ions, leading to the layers shorting out. A possible material that might be used is nickel, which exhibits a much lower mobility than silver [37]. Using a nickel epoxy would still suffer the same problems with aligning the layers and would need a new manufacturing procedure. The current procedure for the CA specimens calls for the specimens to be connected with epoxy as the layers are stacked on the alignment jig (Figure 21) to achieve the arraignment shown in Figure 20. This presents problems with methods similar to that of the SE specimens because, to be constructed this

way, two separate types of epoxy would be applied in the same interfaces at the same time. The simultaneous application of two different types of epoxy was tested with the SE specimens and the silver epoxy was shown to diffuse into the medical grade epoxy, yielding the method untenable. It might be possible to stack the layers as such but only use the nickel epoxy and not the medical grade epoxy used to connect the layers. Once cured, the layers should be very parallel to each other with electrical connectivity established but mechanically connection would only be at the copper tape-layer interfaces. The medical grade epoxy could then be injected between the layers to fully mechanically connect the layers and allow for the even distribution of stress during loading. More specimens must be made and tested in order to determine whether this method would work. Testing should follow the same parameters that were used in this study (2 Hz frequency, 500 N mechanical load, 38 resistance load sweep) to allow proper comparison of results.

References

- [1] Lisa. A Pruitt, A. M. C., 2011, "Mechanics of Biomaterials: Fundamental Principles for Implant Design," University Press, Cambridge, United Kingdom, pp. 456-457.
- [2] "National Institute of Neurological Disorders and Stroke: Low Back Pain Fact Sheet, 2011."
- [3] Kurtz, S., Edidin, A.A., 2006, Spine Technology Handbook, Elsevier Academic Press, Burlington, MA.
- [4] Zdeblick, T. A., and Phillips, F. M., 2003, "Interbody cage devices," Spine, 28(15S), pp. S2-S7.
- [5] KANE, W. J., 1988, "Direct current electrical bone growth stimulation for spinal fusion," Spine, 13(3), pp. 363-365.
- [6] Gan, J. C., and Glazer, P. A., 2006, "Electrical stimulation therapies for spinal fusions: current concepts," European Spine Journal, 15(9), pp. 1301-1311.
- [7] Spine-Health, 2009, "Spinal Fusion Surgery Worth the Cost for Stenosis Patients," <http://www.spine-health.com/blog/spinal-fusion-surgery-worth-cost-stenosis-patients>.
- [8] Boden, S. D., Zdeblick, T. A., Sandhu, H. S., and Heim, S. E., 2000, "The use of rhBMP-2 in interbody fusion cages: definitive evidence of osteoinduction in humans: a preliminary report," Spine, 25(3), pp. 376-381.
- [9] Gautschi, O. P., Frey, S. P., and Zellweger, R., 2007, "Bone morphogenetic proteins in clinical applications," ANZ journal of surgery, 77(8), pp. 626-631.
- [10] Burkus, J. K., Gornet, M. F., Dickman, C. A., and Zdeblick, T. A., 2002, "Anterior lumbar interbody fusion using rhBMP-2 with tapered interbody cages," Journal of spinal disorders & techniques, 15(5), pp. 337-349.
- [11] Haid Jr, R. W., Branch Jr, C. L., Alexander, J. T., and Burkus, J. K., 2004, "Posterior lumbar interbody fusion using recombinant human bone morphogenetic protein type 2 with cylindrical interbody cages," The Spine Journal, 4(5), pp. 527-538.
- [12] Fukada, E., and Yasuda, I., 1957, "On the piezoelectric effect of bone," Journal of the Physical Society of Japan, 12(10), pp. 1158-1162.
- [13] Simon, J., and Simon, B., 2008, "Electrical bone stimulation," Musculoskeletal Tissue Regeneration, Springer, pp. 259-287.
- [14] Bodamyali, T., Bhatt, B., Hughes, F., Winrow, V., Kanczler, J., Simon, B., Abbott, J., Blake, D., and Stevens, C., 1998, "Pulsed Electromagnetic Fields Simultaneously Induce Osteogenesis and Upregulate Transcription of Bone Morphogenetic Proteins 2 and 4 in Rat Osteoblasts *in Vitro*," Biochemical and biophysical research communications, 250(2), pp. 458-461.
- [15] Kahanovitz, N., 2002, "Electrical stimulation of spinal fusion: a scientific and clinical update," The Spine Journal, 2(2), pp. 145-150.
- [16] Shellock, F. G., Hatfield, M., Simon, B. J., Block, S., Wamboldt, J., Starewicz, P. M., and Punched, W. F., 2000, "Implantable spinal fusion stimulator: assessment of MR safety and artifacts," Journal of Magnetic Resonance Imaging, 12(2), pp. 214-223.
- [17] Friedenber, Z., Zemsky, L., and Pollis, R., 1974, "The response of non-traumatized bone to direct current," The Journal of Bone & Joint Surgery, 56(5), pp. 1023-1030.
- [18] Toth, J. M., Seim III, H. B., Schwardt, J. D., Humphrey, W. B., Wallskog, J. A., and Turner, A. S., 2000, "Direct current electrical stimulation increases the fusion rate of spinal fusion cages," Spine, 25(20), pp. 2580-2587.
- [19] Dejardin, L. M., Kahanovitz, N., Arnoczky, S. P., and Simon, B. J., 2001, "The effect of varied electrical current densities on lumbar spinal fusions in dogs," The Spine Journal, 1(5), pp. 341-347.
- [20] Simon, B. J., and Schwardt, J. D., 2001, "Direct current stimulation of spinal interbody fixation device," Google Patents.
- [21] Baranowski Jr, T. J., and Black, J., 1987, "The mechanism of faradic stimulation of osteogenesis," Mechanistic Approaches to Interactions of Electric and Electromagnetic Fields With Living Systems, Springer, pp. 399-416.

- [22] Bodamyali, T., Kanczler, J., Simon, B., Blake, D., and Stevens, C., 1999, "Effect of faradic products on direct current-stimulated calvarial organ culture calcium levels," *Biochemical and biophysical research communications*, 264(3), pp. 657-661.
- [23] Bassett, C. A. L., and Herrmann, I., 1961, "Influence of oxygen concentration and mechanical factors on differentiation of connective tissues in vitro."
- [24] Arnett, T., and Spowage, M., 1996, "Modulation of the resorptive activity of rat osteoclasts by small changes in extracellular pH near the physiological range," *Bone*, 18(3), pp. 277-279.
- [25] Fredericks, D. C., Smucker, J., Petersen, E. B., Bobst, J. A., Gan, J. C., Simon, B. J., and Glazer, P., 2007, "Effects of direct current electrical stimulation on gene expression of osteopromotive factors in a posterolateral spinal fusion model," *Spine*, 32(2), pp. 174-181.
- [26] Abdou, M., 2007, "Use of Carbon Nanotubes in the Manufacture of Orthopedic Implants," Google Patents.
- [27] Hyer, M. W., 2009, *Stress analysis of fiber-reinforced composite materials*, DEStech Publications, Inc.
- [28] Pogany, G., 1969, "The β -relaxation in epoxy resins; the temperature and time-dependence of cure," *Journal of materials science*, 4(5), pp. 405-409.
- [29] Jeong, U., Ryu, D., Kim, J., Kim, D., Russell, T. P., and Hawker, C. J., 2003, "Volume contractions induced by crosslinking: a novel route to nanoporous polymer films," *Advanced Materials*, 15(15), pp. 1247-1250.
- [30] Mohammadi, F., Khan, A., and Cass, R. B., "Power generation from piezoelectric lead zirconate titanate fiber composites," *Proc. Materials Research Society Symposium Proceedings*, Cambridge Univ Press, pp. 263-270.
- [31] Jaffe, B., Cook, W. R., Jaffe, H., 1971, *Piezoelectric ceramics*, New York: Academic.
- [32] Law, H., Rossiter, P., Simon, G., and Unsworth, J., 1995, "A model for the structural hysteresis in poling and thermal depoling of PZT ceramics," *Journal of materials science*, 30(19), pp. 4901-4905.
- [33] Platt, S. R., Farritor, S., and Haider, H., 2005, "On low-frequency electric power generation with PZT ceramics," *Mechatronics, IEEE/ASME Transactions on*, 10(2), pp. 240-252.
- [34] Swallow, L., Luo, J., Siores, E., Patel, I., and Dodds, D., 2008, "A piezoelectric fibre composite based energy harvesting device for potential wearable applications," *Smart Materials and Structures*, 17(2), p. 025017.
- [35] Luchaninov, A., Shil'nikov, A., Shuvalov, L., and Malyshev, V., 1993, "The effect of mechanical stress on the properties of electrically depolarized piezoelectric ceramics," *Ferroelectrics*, 145(1), pp. 235-239.
- [36] Zhang, Q. M., and Zhao, J., 1999, "Electromechanical properties of lead zirconate titanate piezoceramics under the influence of mechanical stresses," *Ultrasonics, Ferroelectrics and Frequency Control, IEEE Transactions on*, 46(6), pp. 1518-1526.
- [37] Wales, U. o. S., 2003, "Ionic Mobility Tables," http://web.med.unsw.edu.au/phbsoft/mobility_listings.htm.
- [38] Hutton, W., Cyron, B., and Stott, J., 1979, "The compressive strength of lumbar vertebrae," *Journal of anatomy*, 129(Pt 4), p. 753.
- [39] Epo-tek, 2014, "Medical Brochure," http://www.epotek.com/site/files/brochures/pdfs/medical_brochure.pdf.
- [40] SmartMaterials, 2014, "PZT Materials," <http://www.smart-material.com/PZTFiber-product-main.html>.
- [41] Victrex, 2014, "Victrex PEEK Polymers," <http://www.victrex.com/en/products/victrex-peek-polymers/victrex-peek-polymers.php>
- [42] Walpole, S. C., Prieto-Merino, D., Edwards, P., Cleland, J., Stevens, G., and Roberts, I., 2012, "The weight of nations: an estimation of adult human biomass," *BMC Public Health*, 12(1), p. 439.
- [43] Kumar, N., Judith, M. R., Kumar, A., Mishra, V., and Robert, M. C., 2005, "Analysis of stress distribution in lumbar interbody fusion," *Spine*, 30(15), pp. 1731-1735.

Appendix A: Methods and Materials

Electrode (cathode) Choice:

We used titanium wire for our cathode instead of a material like stainless steel. We chose titanium because titanium wires are very successful with delivering a constant current across the length of the electrode, whereas it has been found that stainless steel wire doesn't distribute its current uniformly. Instead most of the current leaves from the first connection to tissue which occurs at the insulation and wire connection, causing a much higher current density in a specific location which can lead to osteonecrosis [19].

Epoxy Types and Reason for Picking:

After trying multiple different materials, we chose to use EPO-TEK epoxy type 301 for the base of our composite. We chose this epoxy for multiple reasons. First, its compressive strength was high enough that we are confident compressive failure won't occur during loading of the spine. Vertebrae have an average compressive breaking load of 6,475 N [38]. We performed a standard compression test on the epoxy specimen and found its ultimate strength to be in excess of 10,000 N. With the results from our test, we can be confident that loading through the spine won't cause our device to fail or lose its mechanical integrity. Second, the EPO-TEK type 301 epoxy is a medical grade epoxy that is commonly used for molding medical implants and for many types of encapsulation [39]. Biocompatibility is very important because if the composite matrix reacts negatively with the body, bone healing would be impeded as well as increasing the potential for necrosis in the surrounding area. Finally, the epoxy can be cured at low temperatures, even at room temperature. Room temperature curing allows the setting out epoxy without coming close to exceeding the Curie temperature of piezoelectric materials. The Curie temperature is the point at which the electrical polarization achieved during poling is reversed. The kind

of PZT we used was 5A1, which has a Curie temperature of 335 degrees Celsius [40]. PEEK was not picked for the base of our composite as it has a melting temperature of around 370 degrees Celsius which could interfere with our poled specimens [41].

Fiber Decision

Lead Zirconate Titanate (PZT) is a commonly use piezoelectric ceramic for applications such as electromechanical sensors and generators.[31] The specific type of PZT, PZT-5A1 was chosen due to its high d_{33} value (440×10^{-12} m/V) and because fibers of the geometry and length that we desired could be purchased in the form of PZT-5A1 from Smart Materials Inc.

Manufacturing Process

The manufacturing process begins with the creation of a composite matrix column which can be sliced with a diamond saw to create the correct thickness layers for the specimens. To create the composite column, a customized stainless steel mold was created. The mold was machined to the exact dimensions of the specimen with enough height to allow a 100mm tall specimen to be created at once. The assembled mold is seen in Figure 18.

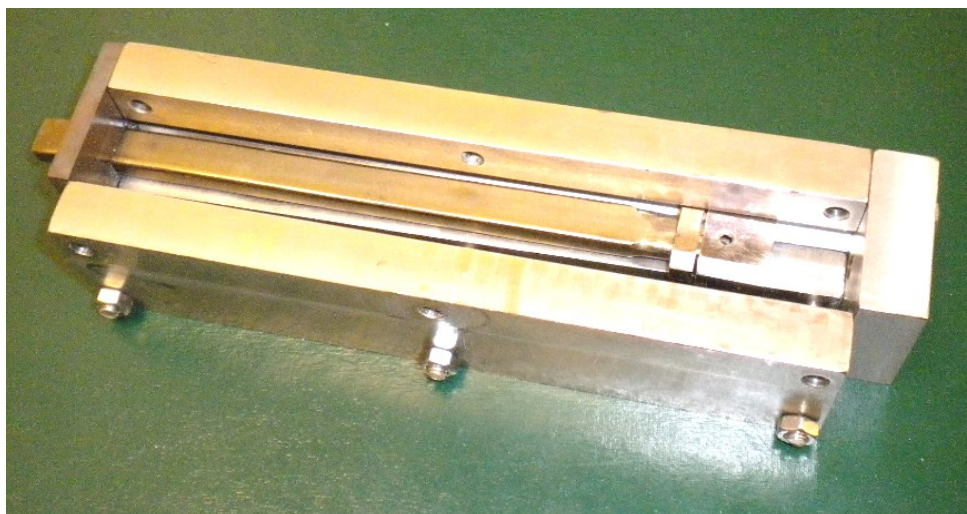


Figure 18: Assembled composite matrix column mold showing inside workings

Before the parts of the mold are assembled, a mold release agent is applied to the inside surfaces to allow an easier removal of the column from the mold. After the parts of the mold are assembled, the fibers are introduced. The mold was designed to provide alignment with the use of 1mm diameter holes on the top and bottom which the fibers are hand-fed through. The holes, seen in Figure 19, are evenly distributed across the surface to reduce the chance of fibers interfering with each other.

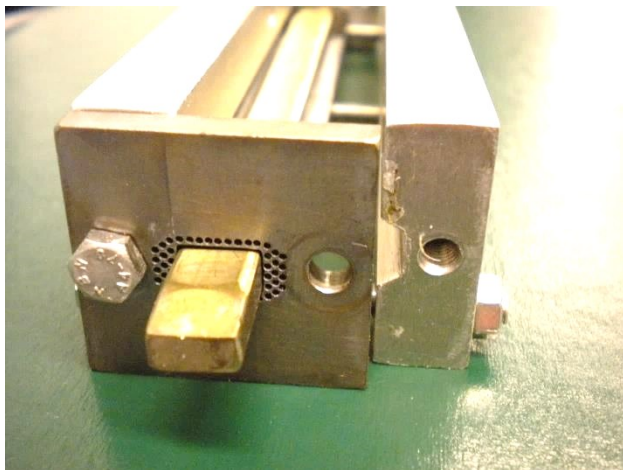


Figure 19: Top view of the assembled column mold

Once the fibers have been aligned, a two-part medical grade epoxy is injected through a slot in the top part of the mold until the entire volume is filled. The epoxy is allowed 24 hours to cure at room temperature and is then removed from the mold. The ends of the column are then faced off to prepare the specimen for slicing on the diamond saw. After the 3 mm thick slices are cut, the outside and inside surfaces of the layers are covered with tape, leaving the top and bottom surfaces uncovered. A 100 nm thick gold electrode was sputter-coated on the top and bottom of the slices to provide electrical connection across each surface, touching the ends of the fibers. The tape was removed and the specimen slices were prepared for layering by removing any extra gold that wandered from the desired location to eliminate chances for the specimen to short across the layers. The slices are then electrically connected in parallel and mechanically connected in series as seen in Figure 20.



Figure 20: Side view of the specimen, detailing the design for electrical connection (black)

One method of manufacturing used copper tape with conductive adhesive (CA) to electrically connect the layers. Epoxy was used to mechanically connect the layers of the generator. The other method also used epoxy to mechanically connect the layers but used silver epoxy (SE) to provide the electrical connection from copper tape to the gold electrodes on the slices. The slices were stacked on an alignment jig (Figure 21) during the application of epoxy and were allowed to cure for 24 hours at room temperature.

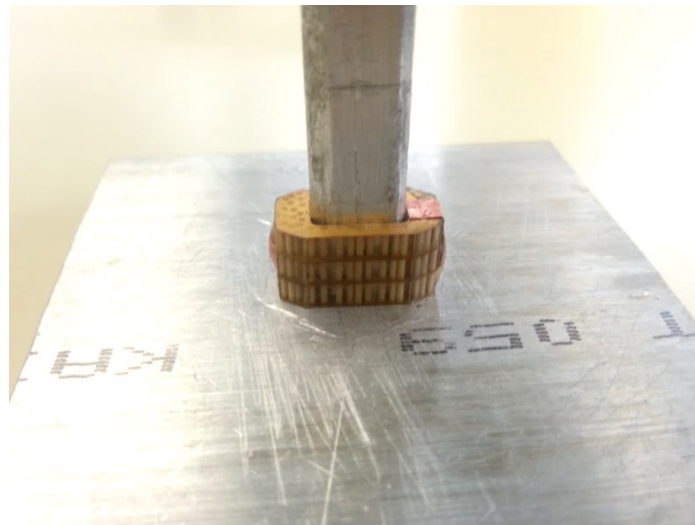


Figure 21: Alignment jig providing support to a stacked specimen while curing

After the epoxy was cured, the stacked specimen was removed from the jig and was put through a poling process. To pole the piezoelectric elements, the specimen was placed between two electrically charged platens, one positive and one negative, and an electric field of 1 kV/mm was applied for 30 minutes. After a 30 minute rest time the specimen was placed in a MTS Model 858 Mini Bionix II with a

self-aligning platen for cyclic compression testing. The full testing regimen consisted of 3 separate tests: After being cured at room temperature (RTC), after a heat curing (HC), and after being encapsulated (ENC). The SE specimens required a heat treatment to cure the silver epoxy (120°C for 1 hour) and therefore was not able to have a RTC test performed. For the CA specimens, a heat treatment of 65°C was applied for at least 1 hour. After the HC test was conducted, the specimens had wires attached to the positive and negative terminals on the specimen. By doing this, the specimens can to be poled after being encapsulated with another coat of epoxy. Using a customized encapsulation mold a .5 mm thick layer of epoxy was added to the specimens while also adding volume to one end to allow room for a surgical tool to attach to the specimen for implanting. The transformation from HC to ENC can be seen in Figure 22. After the specimens were encapsulated, a final poling procedure was administered and the final test, ENC, was conducted.



Figure 22: Comparison of an initial specimen (left) and an encapsulated specimen

The electromechanical testing conditions for each specimen were identical. The specimen was subjected to a cyclic load of 500 N with a frequency of 2 Hz across a range of 38 resistance loads. The mechanical load and frequency were chosen as they closely modeled on an average adults walking gait and load applied through the spine [42, 43]. Figure 23 displays an example of the output from the full

testing regimen. By performing a resistance sweep, the load resistance where peak power occurs can be obtained, allowing the impedance of the specimen to be projected.

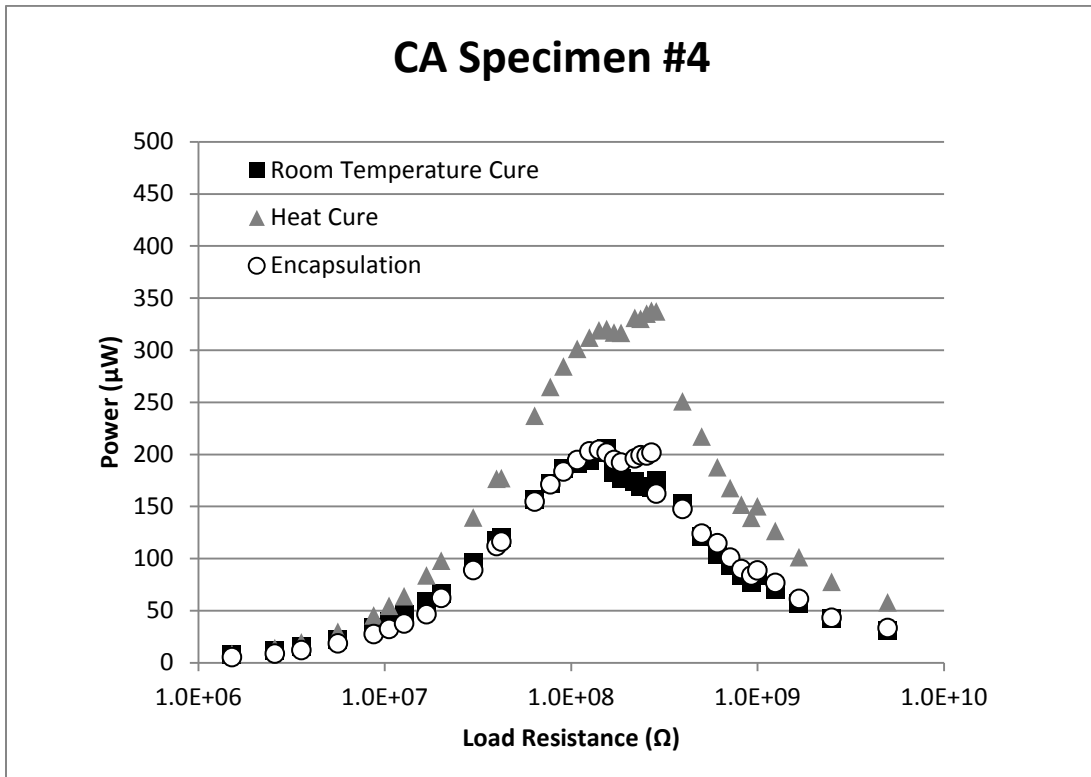


Figure 23: Power output for the 4th conductive adhesive (CA) method specimen across the full testing regimen